



Contents lists available at ScienceDirect

# Spectrochimica Acta Part A: Molecular and Biomolecular Spectroscopy

journal homepage: [www.elsevier.com/locate/saa](http://www.elsevier.com/locate/saa)

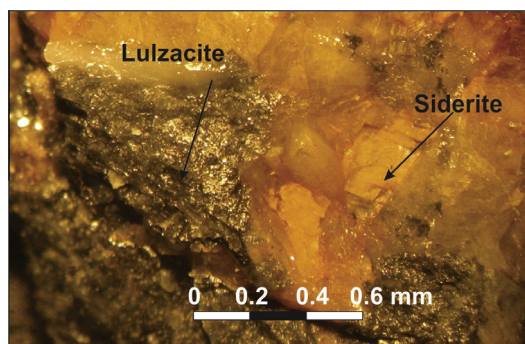
## A vibrational spectroscopic study of the phosphate mineral lulzacite $\text{Sr}_2\text{Fe}^{2+}(\text{Fe}^{2+},\text{Mg})_2\text{Al}_4(\text{PO}_4)_4(\text{OH})_{10}$

Ray L. Frost<sup>a,\*</sup>, Andrés López<sup>a</sup>, Fernanda M. Belotti<sup>b</sup>, Yunfei Xi<sup>a</sup>, Ricardo Scholz<sup>c</sup><sup>a</sup> School of Chemistry, Physics and Mechanical Engineering, Science and Engineering Faculty, Queensland University of Technology, GPO Box 2434, Brisbane, Queensland 4001, Australia<sup>b</sup> Federal University of Itajubá, Campus Itabira, Itabira, MG, Brazil<sup>c</sup> Geology Department, School of Mines, Federal University of Ouro Preto, Campus Morro do Cruzeiro, Ouro Preto, MG 35400-00, Brazil

### HIGHLIGHTS

- We have studied the mineral lulzacite from Saint-Aubin des Chateaux mine, France.
- Using a combination of electron microscopy with EDX and vibrational spectroscopic techniques.
- Chemical analysis shows a Sr, Fe, Al phosphate with minor amounts of Ga, Ba and Mg.
- Vibrational spectroscopy offers insights into the molecular structure of the phosphate mineral lulzacite.

### GRAPHICAL ABSTRACT



### ARTICLE INFO

#### Article history:

Received 6 January 2014  
 Received in revised form 29 January 2014  
 Accepted 9 February 2014  
 Available online 24 February 2014

#### Keywords:

Lulzacite  
 Strontium  
 Phosphate  
 Raman spectroscopy

### ABSTRACT

The mineral lulzacite from Saint-Aubin des Chateaux mine, France, with theoretical formula  $\text{Sr}_2\text{Fe}^{2+}(\text{Fe}^{2+},\text{Mg})_2\text{Al}_4(\text{PO}_4)_4(\text{OH})_{10}$  has been studied using a combination of electron microscopy with EDX and vibrational spectroscopic techniques. Chemical analysis shows a Sr, Fe, Al phosphate with minor amounts of Ga, Ba and Mg. Raman spectroscopy identifies an intense band at  $990\text{ cm}^{-1}$  with an additional band at  $1011\text{ cm}^{-1}$ . These bands are attributed to the  $\text{PO}_4^{3-}$   $\nu_1$  symmetric stretching mode. The  $\nu_3$  anti-symmetric stretching modes are observed by a large number of Raman bands. The Raman bands at 1034, 1051, 1058, 1069 and 1084 together with the Raman bands at 1098, 1116, 1133, 1155 and  $1174\text{ cm}^{-1}$  are assigned to the  $\nu_3$  antisymmetric stretching vibrations of  $\text{PO}_4^{3-}$  and the  $\text{HOPO}_3^{2-}$  units. The observation of these multiple Raman bands in the symmetric and antisymmetric stretching region gives credence to the concept that both phosphate and hydrogen phosphate units exist in the structure of lulzacite. The series of Raman bands at 567, 582, 601, 644, 661, 673 and  $687\text{ cm}^{-1}$  are assigned to the  $\text{PO}_4^{3-}$   $\nu_2$  bending modes. The series of Raman bands at 437, 468, 478, 491,  $503\text{ cm}^{-1}$  are attributed to the  $\text{PO}_4^{3-}$  and  $\text{HOPO}_3^{2-}$   $\nu_4$  bending modes.

No Raman bands of lulzacite which could be attributed to the hydroxyl stretching unit were observed. Infrared bands at  $3511$  and  $3359\text{ cm}^{-1}$  are ascribed to the OH stretching vibration of the OH units. Very broad bands at  $3022$  and  $3299\text{ cm}^{-1}$  are attributed to the OH stretching vibrations of water. Vibrational spectroscopy offers insights into the molecular structure of the phosphate mineral lulzacite.

© 2014 Elsevier B.V. All rights reserved.

\* Corresponding author. Tel.: +61 7 3138 2407; fax: +61 7 3138 1804.

E-mail address: [r.frost@qut.edu.au](mailto:r.frost@qut.edu.au) (R.L. Frost).

## Introduction

The mineral lulzacite is a rare strontium containing phosphate mineral of general chemical formula  $\text{Sr}_2\text{Fe}^{2+}(\text{Fe}^{2+},\text{Mg})_2\text{Al}_4(\text{PO}_4)_4(\text{OH})_{10}$ . The mineral was first described in 2000 from quartzite deposits at Saint-Aubin-des-Châteaux, Loire-Atlantique, France [1]. The mineral occurs with quartz and siderite. Other minerals found with lulzacite include apatite, goyazite and pyrite [2]. Lulzacite is triclinic with *P1* space group, and unit cell parameters are:  $a = 5.457(1)$  Å,  $b = 9.131(2)$  Å,  $c = 9.769(2)$  Å,  $\alpha = 108.47(3)^\circ$ ,  $\beta = 91.72(3)^\circ$  and  $\gamma = 97.44(3)^\circ$  [2]. The mineral is isostructural with jamesite ( $\text{Pb}_2\text{Zn}(\text{Fe}^{2+},\text{Zn})_2\text{Fe}^{3+}_4(\text{AsO}_4)_4(\text{OH})_{10}$ ) [3,4].

Raman spectroscopy has proven most useful for the study of mineral structure. Raman spectroscopy is an important tool in the characterization of phosphates in complex paragenesis [5–8]. In recent years, spectroscopic studies concerning phosphate minerals are increasing, especially due to their industrial and technological importance [8–11]. The aim of this paper is to report the Raman spectra of lulzacite, and to relate the spectra to the molecular structure of this hydrogen-phosphate mineral. The paper follows the systematic research of the large group of secondary minerals and especially molecular structure of minerals containing oxyanions using IR and Raman spectroscopy.

## Experimental

### Samples description and preparation

The lulzacite sample studied in this work forms part of the collection of the Geology Department of the Federal University of Ouro Preto, Minas Gerais, Brazil, with sample code SAC-106. The studied sample is from Saint-Aubin-des-Châteaux, located 8 km west of Châteaubriant (Loire-Atlantique, France). Quartzite forms a sequence of decimetric beds within Armorican sandstones. In the lower southwest part of the quarry, appears a micro-crystalline limestone level about 1 m thick, enriched in pyrite and organic matter. Veinlets filled mainly by quartz, siderite and recrystallised pyrite, with traces of sphalerite and galena, occur at the contact between quartzite and pyrite-rich limestone. Within these veinlets, phosphates are irregularly distributed and forms a complex paragenesis including lulzacite, goyazite, apatite and sulphides (pyrrhotite, pyrite, bournonite, boulangerite, sphalerite, galena and chalcopyrite) [2].

The sample was gently crushed and the associated minerals were removed under a stereomicroscope Leica MZ4. The lulzacite studied in this work occurs in association with siderite. Scanning electron microscopy (SEM) in the EDS mode was applied to support the mineral characterization.

### Scanning electron microscopy (SEM)

Experiments and analyses involving electron microscopy were performed in the Center of Microscopy of the Universidade Federal de Minas Gerais, Belo Horizonte, Minas Gerais, Brazil (<http://www.microscopia.ufmg.br>). Lulzacite massive fragment up to 0.5 mm was coated with a 5 nm layer of evaporated Au. Secondary Electron and Backscattering Electron images were obtained using a JEOL JSM-6360LV equipment. A qualitative and semi-quantitative chemical analysis in the EDS mode was performed with a ThermoNORAN spectrometer model Quest and was applied to support the mineral characterization.

### Raman microprobe spectroscopy

Crystals of lulzacite were placed on a polished metal surface on the stage of an Olympus BHS microscope, which is equipped with

10×, 20×, and 50× objectives. The microscope is part of a Renishaw 1000 Raman microscope system, which also includes a monochromator, a filter system and a CCD detector (1024 pixels). The Raman spectra were excited by a Spectra-Physics model 127 He–Ne laser producing highly polarized light at 633 nm and collected at a nominal resolution of  $2\text{ cm}^{-1}$  and a precision of  $\pm 1\text{ cm}^{-1}$  in the range between 200 and  $4000\text{ cm}^{-1}$ . Repeated acquisitions on the crystals using the highest magnification (50×) were accumulated to improve the signal to noise ratio of the spectra. Raman Spectra were calibrated using the  $520.5\text{ cm}^{-1}$  line of a silicon wafer. The Raman spectrum of at least 10 crystals was collected to ensure the consistency of the spectra.

An image of the lulzacite crystals measured is shown in the supplementary information as Fig. S1. Clearly the crystals of lulzacite are readily observed, making the Raman spectroscopic measurements readily obtainable.

### Infrared spectroscopy

Infrared spectra were obtained using a Nicolet Nexus 870 FTIR spectrometer with a smart endurance single bounce diamond ATR cell. Spectra over the  $4000\text{--}525\text{ cm}^{-1}$  range were obtained by the co-addition of 128 scans with a resolution of  $4\text{ cm}^{-1}$  and a mirror velocity of  $0.6329\text{ cm/s}$ . Spectra were co-added to improve the signal to noise ratio.

Spectral manipulation such as baseline correction/adjustment and smoothing were performed using the Spectralcalc software package GRAMS (Galactic Industries Corporation, NH, USA). Band component analysis was undertaken using the Jandel ‘Peakfit’ software package that enabled the type of fitting function to be selected and allows specific parameters to be fixed or varied accordingly. Band fitting was done using a Lorentzian–Gaussian cross-product function with the minimum number of component bands used for the fitting process. The Gaussian–Lorentzian ratio was maintained at values greater than 0.7 and fitting was undertaken until reproducible results were obtained with squared correlations of  $r^2$  greater than 0.995.

## Results and discussion

### Chemical characterization

The BSE image of lulzacite sample studied in this work is shown in Fig. 1. Qualitative and semi-quantitative chemical composition shows a Sr, Fe, Al phosphate with minor amounts of Ga, Ba and

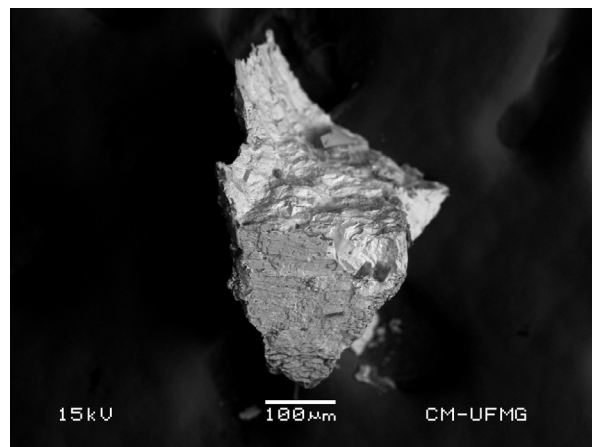


Fig. 1. Backscattered electron image (BSI) of a lulzacite crystal fragment up to 0.5 mm in length.

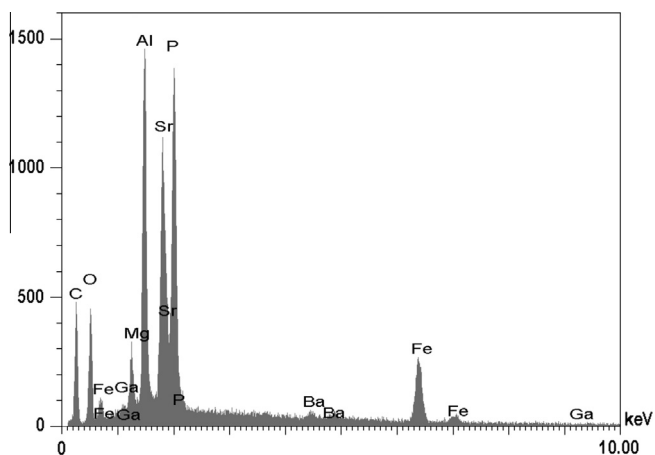


Fig. 2. EDS analysis of lulzacite.

Mg. Carbon was observed due to effect of conductive tape and metallization (see Fig. 2).

The chemical analysis by EMP shows chemical formula expressed by  $\text{Fe}^{2+}\text{Fe}_5^{3+}(\text{PO}_4)_4(\text{OH})_5 \cdot 4\text{H}_2\text{O}$  that indicate predominance of lulzacite member in a triple series between lulzacite, Zn-lulzacite and Al-lulzacite. Minor amount of Al was also found.

### Vibrational spectroscopy

#### Background

In aqueous systems, the Raman spectra of phosphate oxyanions show a symmetric stretching mode ( $\nu_1$ ) at  $938\text{ cm}^{-1}$ ,

an antisymmetric stretching mode ( $\nu_3$ ) at  $1017\text{ cm}^{-1}$ , a symmetric bending mode ( $\nu_2$ ) at  $420\text{ cm}^{-1}$  and a  $\nu_4$  bending mode at  $567\text{ cm}^{-1}$ . S.D. Ross in Farmer (page 404) listed some well-known minerals containing phosphate, which were either hydrated or hydroxylated or both [9]. The vibrational spectrum of the dihydrogen phosphate anion has been reported in Farmer. The  $\text{PO}_2$  symmetric stretching mode occurs at  $1072\text{ cm}^{-1}$  and the POH symmetric stretching mode at  $\sim 878\text{ cm}^{-1}$ . The position of the PO stretching vibration for calcium dihydrogen phosphate is found at  $915\text{ cm}^{-1}$ . The POH antisymmetric stretching mode is at  $947\text{ cm}^{-1}$  and the  $\text{P}(\text{OH})_2$  bending mode at  $380\text{ cm}^{-1}$ . The band at  $1150\text{ cm}^{-1}$  is assigned to the  $\text{PO}_2$  antisymmetric stretching mode. The position of these bands will shift according to the crystal structure of archerite.

### Raman and infrared spectroscopy

The Raman spectrum of lulzacite over the  $100\text{--}4000\text{ cm}^{-1}$  spectral range is displayed in Fig. 3a. This figure shows the position and relative intensities of the Raman bands. It may be observed that there are large parts of the spectrum where no Raman intensity is observed. Thus, the spectrum is subdivided into sections depending upon the type of vibration being examined. It is noted that significant intensity exists in the OH stretching region in the  $2800\text{--}4000\text{ cm}^{-1}$  spectral range, reflecting the number of hydroxyl units in the lulzacite structure. The infrared spectrum of lulzacite over the  $500\text{--}4000\text{ cm}^{-1}$  spectral range is shown in Fig. 3b. This figure displays the position and relative intensity of the infrared bands. As for the Raman spectrum, the infrared spectrum is subdivided into sections based upon the type of vibration being studied.

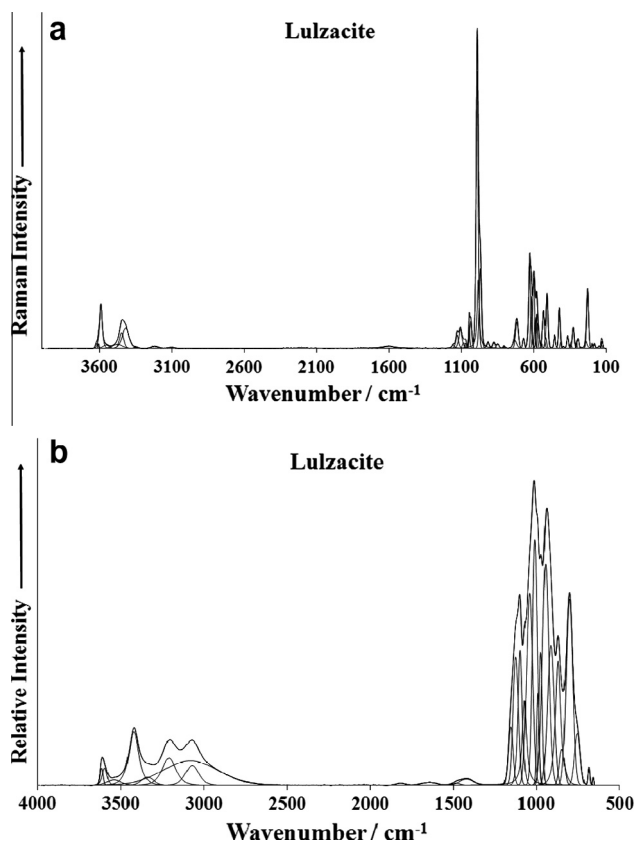


Fig. 3. (a) Raman spectrum of lulzacite (upper spectrum) in the  $100\text{--}1500\text{ cm}^{-1}$  spectral range and (b) infrared spectrum of lulzacite (lower spectrum) in the  $500\text{--}4000\text{ cm}^{-1}$  spectral range.

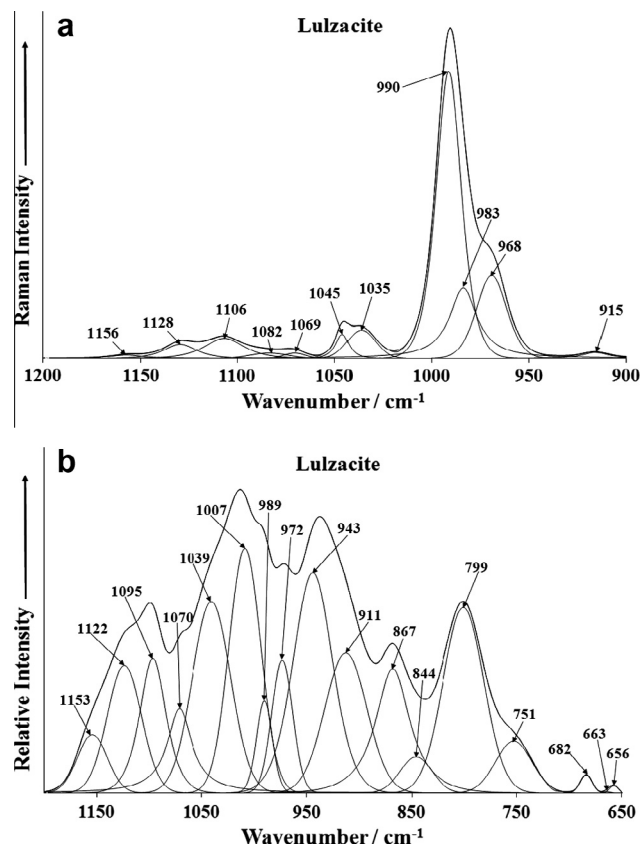


Fig. 4. (a) Raman spectrum of lulzacite (upper spectrum) in the  $900\text{--}1200\text{ cm}^{-1}$  spectral range and (b) infrared spectrum of lulzacite (lower spectrum) in the  $650\text{--}1200\text{ cm}^{-1}$  spectral range.

The Raman spectrum of lulzacite over the 900–1200  $\text{cm}^{-1}$  spectral range is reported in Fig. 4a. The spectrum is dominated by an intense Raman band at 990  $\text{cm}^{-1}$  which is attributed to the  $\text{PO}_4^{3-}$   $\nu_1$  symmetric stretching vibrations. Two shoulder bands are found at 968 and 983  $\text{cm}^{-1}$ . One possibility is that the proton of the hydroxyl unit is mobile and on a picoseconds time scale can transfer to the phosphate units, thus generating a  $\text{HOPO}_3^{2-}$  unit. A Raman band observed at 968  $\text{cm}^{-1}$  is attributed to the PO symmetric stretching vibration of these  $\text{HOPO}_3^{2-}$  units. A series of Raman bands of low intensity are noted at 1035, 1045, 1069, 1082, 1106 and 1128  $\text{cm}^{-1}$ . These bands are assigned to the  $\nu_3$  antisymmetric stretching vibrations of  $\text{PO}_4^{3-}$  and the  $\text{HOPO}_3^{2-}$  units.

The infrared spectrum of lulzacite over the 650–1200  $\text{cm}^{-1}$  spectral range is shown in Fig. 4b. This spectrum is complex and consists of a series of overlapping bands which may be curve resolved into component bands. The infrared bands at 972, 989 and 1007  $\text{cm}^{-1}$  may be assigned to the  $\nu_1$  symmetric stretching vibrations of  $\text{PO}_4^{3-}$  and the  $\text{HOPO}_3^{2-}$  units. The infrared bands at 1070, 1095, 1122 and 1153  $\text{cm}^{-1}$  are assigned to the  $\nu_3$  antisymmetric stretching vibrations of  $\text{PO}_4^{3-}$  and the  $\text{HOPO}_3^{2-}$  units.

The Raman spectrum of lulzacite over the 400–900  $\text{cm}^{-1}$  spectral range is given in Fig. 5a. This figure shows the bands which are due to the bending modes of  $\text{PO}_4^{3-}$  and the  $\text{HOPO}_3^{2-}$  units. The Raman bands at 412, 422 and 455  $\text{cm}^{-1}$  are assigned to the  $\text{PO}_4^{3-}$  and  $\text{HOPO}_3^{2-}$   $\nu_4$  bending modes. The series of Raman bands at 506, 532, 579, 599, 615 and 627  $\text{cm}^{-1}$  are attributed to the  $\text{PO}_4^{3-}$  and  $\text{HOPO}_3^{2-}$   $\nu_2$  bending modes.

A comparison may be based on that with other phosphate containing minerals, which also contain hydroxyl groups. For pseudomalachite  $\text{Cu}_5(\text{PO}_4)_2(\text{OH})_4$ , Raman bands are observed at 482 and 452  $\text{cm}^{-1}$  of about equal intensity. The two  $\nu_2$  bands for

pseudomalachite were reported by Ross [12] at 450 and 422  $\text{cm}^{-1}$ . Cornetite  $\text{Cu}_3(\text{PO}_4)(\text{OH})_3$ , Raman spectra shows an intense band at 433  $\text{cm}^{-1}$  with minor components at 463 and 411  $\text{cm}^{-1}$ . Ross [9] reported two bands at 464 and 411  $\text{cm}^{-1}$  for cornetite. The variation between the spectral results may be attributed to orientation effects and the intensity of different bands will depend on which crystal face is scattering the Raman signal. The Raman spectrum of libethenite  $\text{Cu}_2(\text{PO}_4)(\text{OH})$  showed a single band for  $\nu_2$  at 450  $\text{cm}^{-1}$ . A number of bands in the 480–680  $\text{cm}^{-1}$  region of mineral phosphates were reported by Ross [12] for selected phosphates. Ross attributed these bands to the  $\nu_4$  modes. We observe similar number of bands for the churchite-(Y) minerals. The Raman spectrum of pseudomalachite exhibits bands at 481, 517, 537 and 609  $\text{cm}^{-1}$ . The  $\nu_4$  modes for cornetite were observed at 487, 518, 541 and 570  $\text{cm}^{-1}$ . Bands were observed for libethenite at 556, 582, 626 and 645  $\text{cm}^{-1}$ . These band positions are in good agreement with the values reported by Ross in Farmer's treatise [12]. The Raman spectrum of the far low wavenumber region of lulzacite is shown in Fig. 5b. A strong Raman band is noted at 227  $\text{cm}^{-1}$  which together with other bands in this spectral region are described as lattice vibrations. The Raman bands at 293, 326, 342, 365 and 393 are likely to be associated with metal oxygen stretching vibrations.

The Raman spectrum of lulzacite over the 3000–3700  $\text{cm}^{-1}$  spectral range is reported in Fig. 6a. Two overlapping Raman bands at 3419 and 3447  $\text{cm}^{-1}$  together with the sharp intense Raman band at 3590  $\text{cm}^{-1}$  are assigned to the stretching vibrations of the OH units. The reason for the wide variation of the band position of the hydroxyl units is due to the variation in hydrogen bond strength of these hydroxyl units. The hydroxyl units are non-equivalent. Other low intensity shoulders are observed at 3345, 3554,

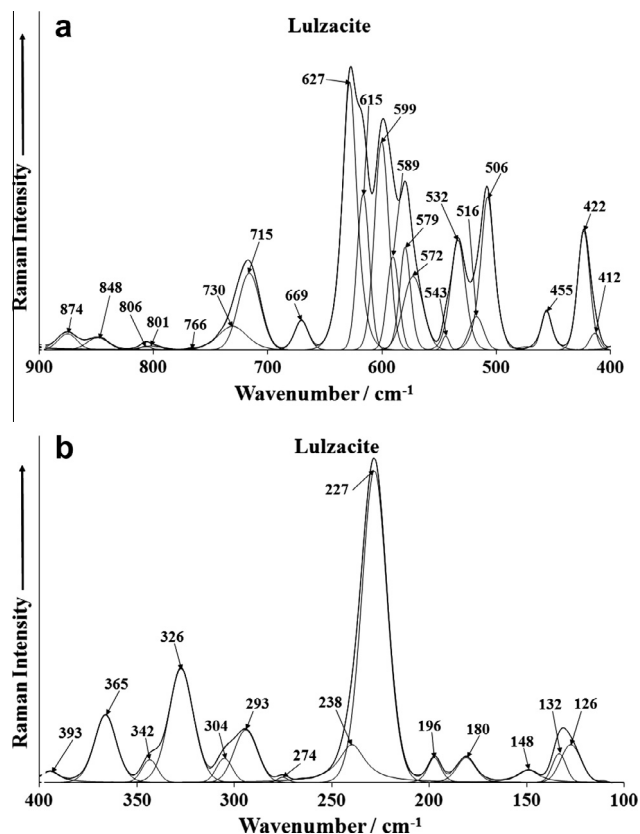


Fig. 5. (a) Raman spectrum of lulzacite (upper spectrum) in the 900–300  $\text{cm}^{-1}$  spectral range and (b) Raman spectrum of lulzacite (lower spectrum) in the 300–100  $\text{cm}^{-1}$  spectral range.

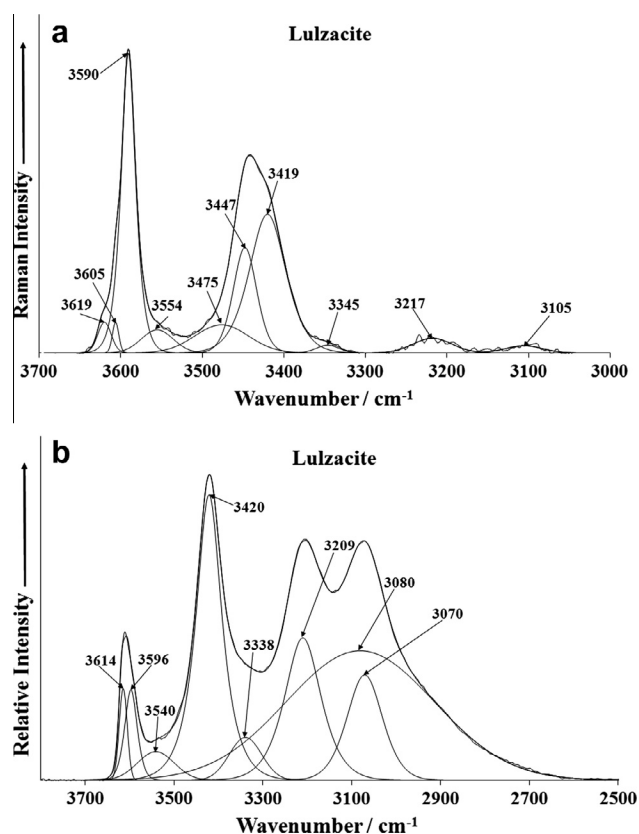


Fig. 6. Raman spectrum of lulzacite (upper spectrum) in the 3000–3700  $\text{cm}^{-1}$  spectral range and Fig. 4b infrared spectrum of lulzacite (lower spectrum) in the 2500–3700  $\text{cm}^{-1}$  spectral range.

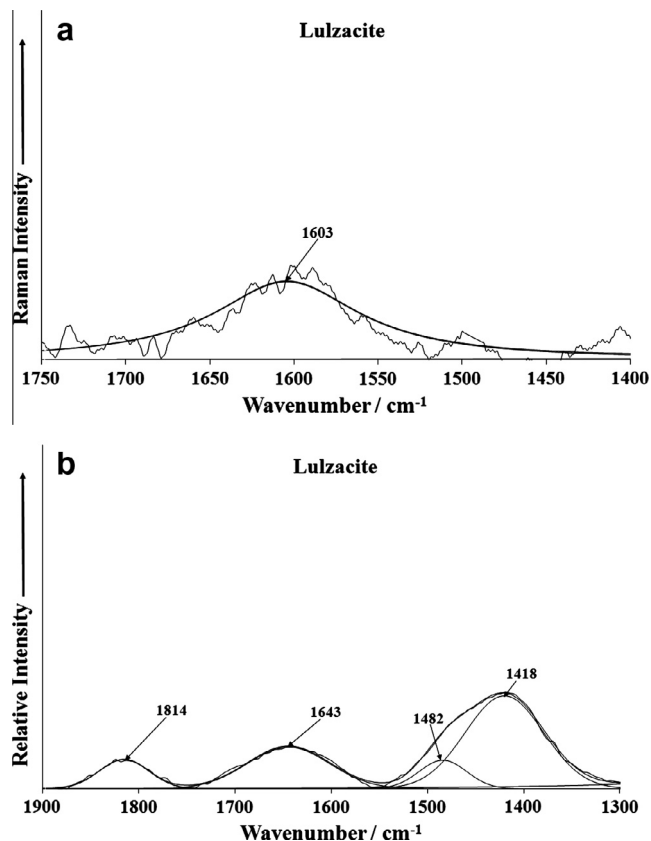


Fig. 7. Raman spectrum of lulzacite (upper spectrum) in the 1400–1750  $\text{cm}^{-1}$  spectral range and Fig. 4b infrared spectrum of lulzacite (lower spectrum) in the 1300–1900  $\text{cm}^{-1}$  spectral range.

3605 and 3619  $\text{cm}^{-1}$ . The low intensity Raman bands at 3105 and 3217  $\text{cm}^{-1}$  maybe due to the stretching vibrations of water. The infrared spectrum of lulzacite over the 2500–3800  $\text{cm}^{-1}$  spectral range is shown in Fig. 6b. The intense infrared bands at 3420, 3596 and 3614  $\text{cm}^{-1}$  are assigned to the stretching vibration of OH units. The broader bands at 3070 and 3209  $\text{cm}^{-1}$  are attributed to water stretching vibrations. The Raman spectrum of lulzacite over the 1400–1750  $\text{cm}^{-1}$  is shown in Fig. 7a. This spectrum suffers from a lack of signal. It is difficult to make a statement about Raman bands being present. The infrared spectrum of lulzacite over the 1300–1900  $\text{cm}^{-1}$  spectral range is reported in Fig. 7b. An infrared band is found at 1643  $\text{cm}^{-1}$  which is ascribed to the bending vibration of strongly bonded water.

## Conclusions

A lulzacite sample was studied by Electron Microscope in the EDS mode, Raman and infrared spectroscopy. The chemical analysis by EMP combined shows chemical formula expressed by  $\text{Fe}^{2+}\text{Fe}_5^{3+}(\text{PO}_4)_4(\text{OH})_5 \cdot 4\text{H}_2\text{O}$  that indicate predominance of lulzacite member in a triple series between lulzacite, Zn-lulzacite and Al-lulzacite. Minor amount of Al was also found.

Raman spectroscopy identifies an intense band at 990  $\text{cm}^{-1}$  and 1011  $\text{cm}^{-1}$ . These bands are attributed to the  $\text{PO}_4^{3-}$   $\nu_1$  symmetric stretching mode. The  $\nu_3$  antisymmetric stretching modes are observed by a large number of Raman bands. The Raman bands at

1034, 1051, 1058, 1069 and 1084 together with the Raman bands at 1098, 1116, 1133, 1155 and 1174  $\text{cm}^{-1}$  are assigned to the  $\nu_3$  antisymmetric stretching vibrations of  $\text{PO}_4^{3-}$  and the  $\text{HOPO}_3^{2-}$  units. The observation of these multiple Raman bands in the symmetric and antisymmetric stretching region gives credence to the concept that both phosphate and hydrogen phosphate units exist in the structure of lulzacite. At least on the picoseconds time scale, the hydrogen phosphate units exist and may be identified by vibrational spectroscopy. The infrared spectrum shows complexity with many overlapping bands. The series of Raman bands at 567, 582, 601, 644, 661, 673 and 687  $\text{cm}^{-1}$  are assigned to the  $\text{PO}_4^{3-}$   $\nu_2$  bending modes. The series of Raman bands at 437, 468, 478, 491, 503  $\text{cm}^{-1}$  are attributed to the  $\text{PO}_4^{3-}$  and  $\text{HOPO}_3^{2-}$   $\nu_4$  bending modes. This work brings into question the actual formula of lulzacite  $\text{Sr}_2\text{Fe}^{2+}(\text{Fe}^{2+}, \text{Mg})_2\text{Al}_4(\text{PO}_4)_4(\text{OH})_{10}$ . The formula should include some hydrogen phosphate units.

Two overlapping Raman bands at 3419 and 3447  $\text{cm}^{-1}$  together with the sharp intense Raman band at 3590  $\text{cm}^{-1}$  are assigned to the stretching vibrations of the OH units. Infrared bands at 3511 and 3359  $\text{cm}^{-1}$  are ascribed to the OH stretching vibration of the OH units. Very broad bands at 3022 and 3299  $\text{cm}^{-1}$  are attributed to the OH stretching vibrations of water. Vibrational spectroscopy offers insights into the molecular structure of the phosphate mineral lulzacite.

## Acknowledgements

The financial and infra-structure support of the Discipline of Nanotechnology and Molecular Science, Science and Engineering Faculty of the Queensland University of Technology, is gratefully acknowledged. The Australian Research Council (ARC) is thanked for funding the instrumentation. The authors would like to acknowledge the Center of Microscopy at the Universidade Federal de Minas Gerais (<http://www.microscopia.ufmg.br>) for providing the equipment and technical support for experiments involving electron microscopy.

## Appendix A. Supplementary data

Supplementary data associated with this article can be found, in the online version, at <http://dx.doi.org/10.1016/j.saa.2014.02.041>.

## References

- [1] Y. Moelo, B. Lasnier, P. Palvadeau, P. Leone, F. Fontan, *Comptes Rendu* 330 (2000) 317–324.
- [2] P. Leone, P. Palvadeau, Y. Moelo, *Comptes Rendu* 3 (2000) 301–308.
- [3] Y. Moelo, O. Rouer, M. Bouhnik-Le Coz, *Eur. J. Mineral.* 20 (2008) 205–216.
- [4] P. Keller, H. Hess, P.J. Dunn, *Chem. Erde* 40 (1981) 105–109.
- [5] M. Łodziński, M. Sitarz, *J. Mol. Struct.* 924–926 (2009) 442–447.
- [6] R.L. Frost, Y. Xi, R. Scholz, F.M. Belotti, M.C. Filho, *J. Mol. Struct.* 1033 (2013) 258–264.
- [7] R.L. Frost, R. Scholz, A. Lopes, Y. Xi, Z.Z. Gobac, L.F.C. Horta, *Spectrochim. Acta A116* (2013) 491–496.
- [8] R.L. Frost, A. Lopez, Y. Xi, A. Granja, R. Scholz, *Spectrochim. Acta A115* (2013) 22–25.
- [9] L.A.d.S. Costa, C. Souza de Miranda, M.I. Campos, D.d.J. Assis, J.I. Druzian, *Rev. GEINTEC* 3 (2013) 055–069.
- [10] J. Jimenez-Guzman, L. Gomez-Ruiz, M. Garcia-Garibay, *Informacion Tecnologica* 14 (2003) 7–12.
- [11] K.C. Sekhar, C.T. Kamala, N.S. Chary, A.B. Mukherjee, *Trace Metals Other Contam. Environ.* 9 (2007) 315–337.
- [12] V.C. Farmer, *Mineralogical Society Monograph 4: The Infrared Spectra of Minerals*, The Mineralogical Society, London, 1974.